SUPPLEMENTARY INFORMATION

Sorting ring polymers by knot type with modulated nanochannels

M. Marenda,[1] E. Orlandini,[2] and C. Micheletti[1]

[1]*SISSA, International School for Advanced Studies, via Bonomea 265, I-34136 Trieste, Italy*
[2]*Dipartimento di Fisica e Astronomia "Galileo Galilei", sezione CNISM, Università degli Studi di Padova, via Marzolo 8, I-35131 Padova, Italy*

I. STOCHASTIC MOTION WITHIN AND ACROSS CHAMBERS

The stochastic motion of rings inside modulated channel displays two regimes: an intra-chamber one at short timescales, and an inter-chamber one at longer timescales. The two regimes are aptly illustrated in Fig S1a which portrays the time dependence of the mean square displacement (MSD) of the center of mass of a ring with $N = 100$ beads inside a single isolated, walled chamber and inside the "infinitely" extended modulated channel and inside.

In the first case, the MSD plateaus at time lags larger than $\sim 2000\tau_{LJ}$, which therefore identifies the characteristic intra-chamber exploration time for the ring and hence the onset of the inter-chamber diffusive regime. The chamber exploration time clearly increases with the chamber size, see panel (b).

In the latter case the asymptotic longitudinal motion is well-consistent with normal diffusion. Fig. S2 shows this regime for two different chain lengths and three different topologies. The uniform channel case is shown as a reference.

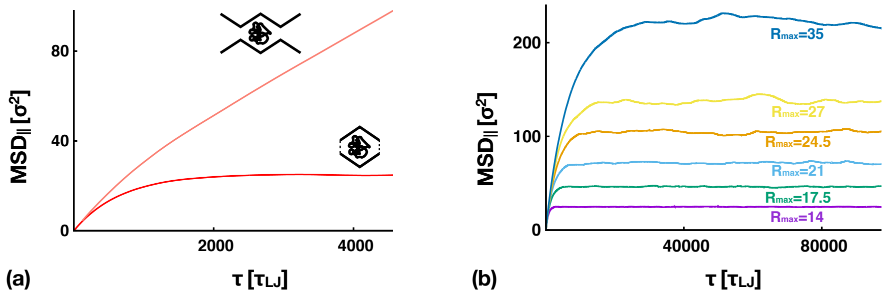

FIG. S1: (a) Longitudinal mean square displacement (MSD) as a function of the time lag for an unknotted chain of $N = 100$ beads. The light-red curve represents the MSD of the ring in the periodically-modulated channel. The red curve instead represents the MSD for the chain trapped inside a single isolated (i.e. walled) chamber of the modulated channel. The same quantity is shown in panel (b) for walled chambers with different values of R_{max}.

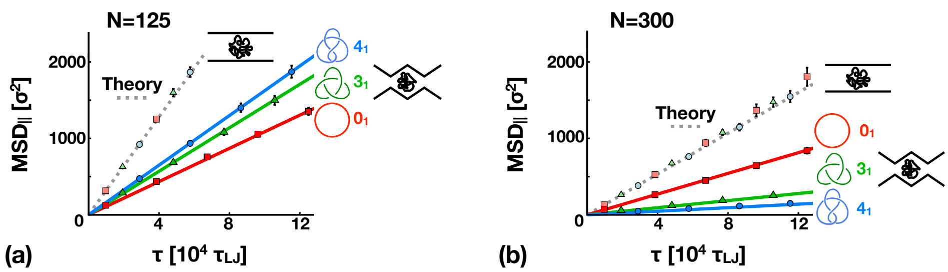

FIG. S2: Mean square longitudinal displacement $MSD_{||}$ versus time lag, τ, for chains of (a) 125 beads and (b) 300 beads and different topologies: 0_1, 3_1 and 4_1. Averages are taken over 10 independent trajectories. The solid lines are direct proportionality best fits for modulated channel data (saturated colors). The dashed line is the theoretical dependence, $D_0 = 2\sigma^2/N\tau_{LJ}$, for the uniform channel case (light colors).

II. LONGITUDINAL EXTENSION OF THE RINGS

The average span of knotted and unknotted rings is shown in Fig. S3a as a function of N. The standard deviations of the span presents oscillations as a function of N that correlate with the oscillation of D/D_0. The quantities present noticeable deviations from the uniform channel case (dotted lines) for lengths $N > 350$, which are long enough to straddle more than one chamber. This emerges clearly from Fig. S4 which shows the probability with which rings of different topologies and lengths occupy 1, 2 or 3 chambers.

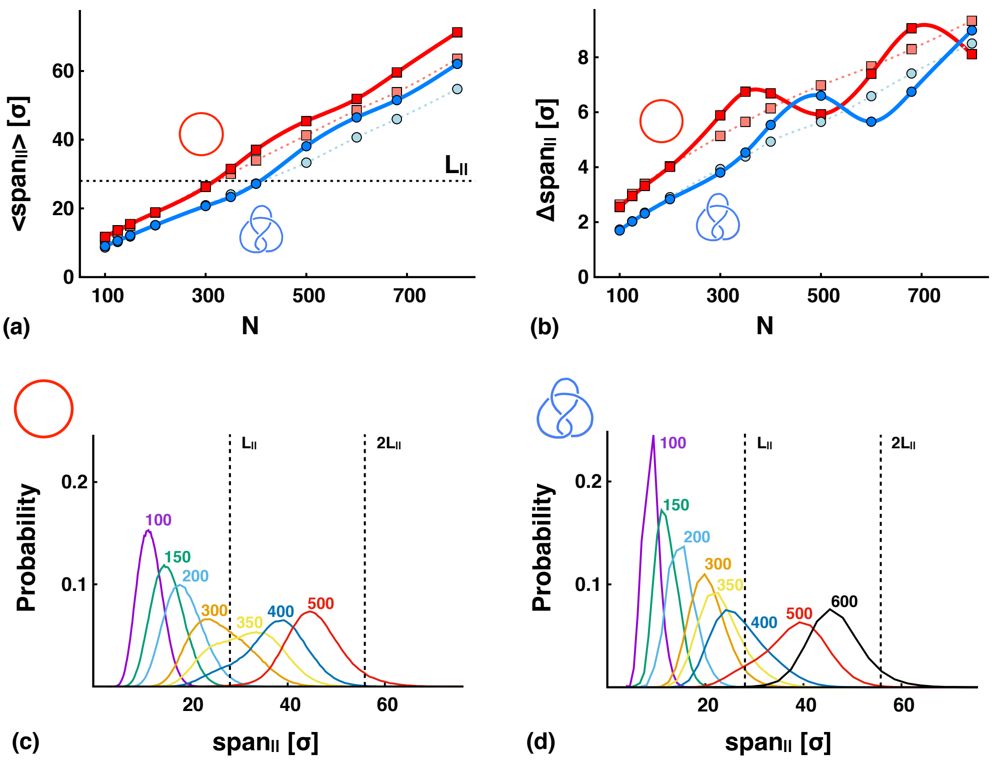

FIG. S3: Average (a) and standard deviation (b) of the longitudinal span of knotted and unknotted rings in modulated nanochannels as a function of N. Data for uniform channels are shown with dashed lines. Probability distributions of the longitudinal span of unknotted and knotted rings for different values of N are shown in panels (c) and (d). The dashed lines mark the values for $L_{||}$ and $2L_{||}$.

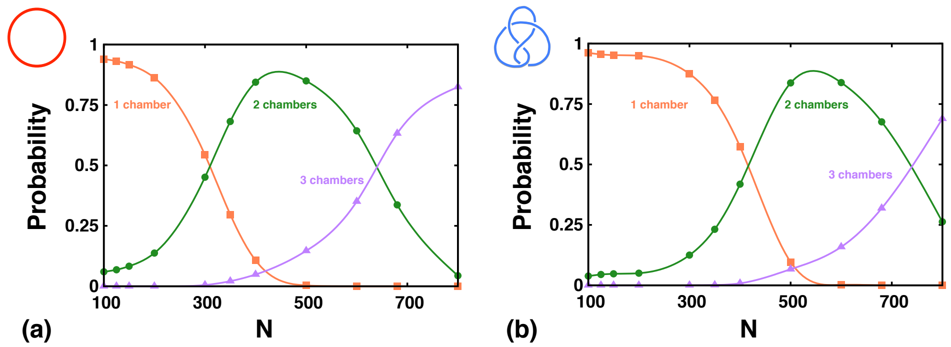

FIG. S4: Probability distribution that a ring occupies 1 chamber (orange curve), 2 chambers (green curve) or 3 chambers (violet curve). The data probabilities are shown as a function of N for both unknotted (a) and 4_1-knotted rings (b). The number of occupied chambers is calculated conservatively by neglecting cases where the longitudinal protrusions into the chambers are less than $L_{||}/10$.

III. SIZE OF THE KNOTTED PORTION AND IMPLICATIONS FOR THE DIFFUSIVE HINDRANCE

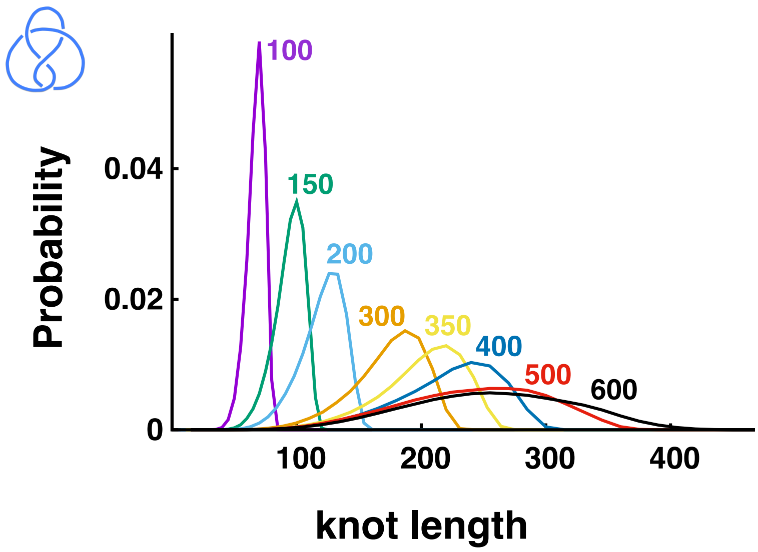

FIG. S5: (a) Probability distribution of the contour length of the knotted region of 4_1 knotted rings of N beads inside modulated channels. The knot length was computed with the minimally-interfering scheme inroduced in ref. [1]. Similarly, to the well-studied case of unconstrained chains [1–3], the average knot contour length increases with N.

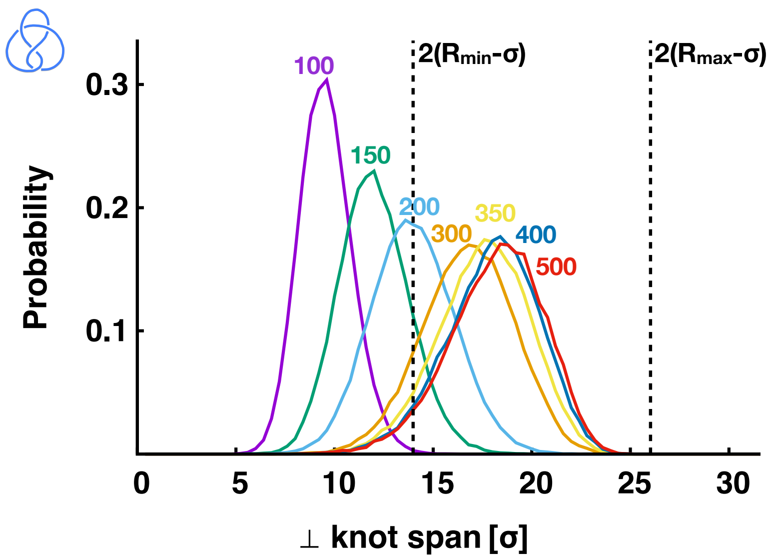

FIG. S6: Probability distribution of the transverse knot span (i.e. the transverse calliper size of the knotted region) for 4_1-knotted rings with $100 \leq N \leq 500$. The two dashed lines indicate the effective maximum and minimum transverse diameters of the modulate chamber. For $N > 200$ most configurations have a knot transverse size larger than the constriction connecting two chamber.

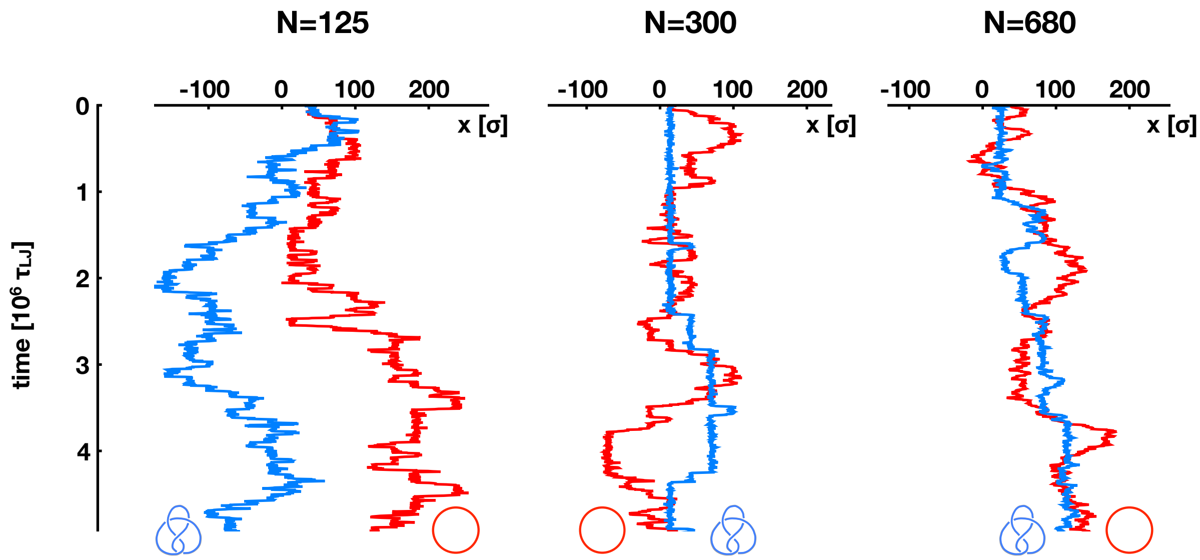

FIG. S7: Trajectories of the longitudinal CoM displacement of rings with $N = 125$, 300 and 680 beads and two different topologies (unknotted in red and figure-of-eight in blue). The hindrance to pore translocation introduced by knots for $N = 300$ and 680 is reflected in the longer intra-chamber dwelling times compared to unknotted rings with same lengths.

IV. DEPENDENCE OF THE DIFFUSION COEFFICIENT ON THE PORE SIZE R_{min}.

We considered rings of $N = 100$ beads and profiled the dependence of the normalised diffusion coefficient, D/D_0 on the width of the channel constriction, R_{min}. The results are shown in Fig. S8 for R_{min} ranging from 4σ to 14σ. The latter corresponds to the uniform channel case because $R_{max} = L_{||}/2 = 14\sigma$, and in fact the $D/D0$ curves for both topologies approach 1 in this limit. The dashed lines indicate the Fick-Jacobs (FJ) theoretical estimates for rings of $N = 100$ beads, which are in good agreement with the actual data.

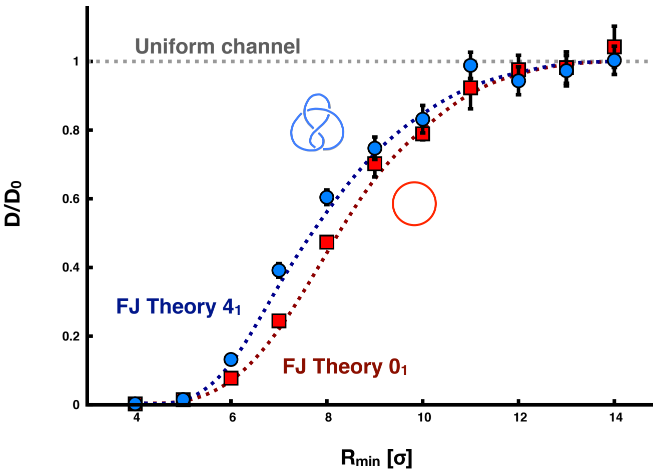

FIG. S8: Normalized diffusion coefficient D/D_0 as a function of the pore radius R_{min} for rings with $N = 100$ beads and two different topologies, unknotted (red squares) and figure-of-eight (blue circles) knotted rings. Dark-red and dark-blue dashed lines are the diffusion coefficients of the rings calculated using the Fick-Jacobs approximation.

V. KNOT LENGTH DURING TRANSLOCATION FOR A DRIVEN DYNAMICS

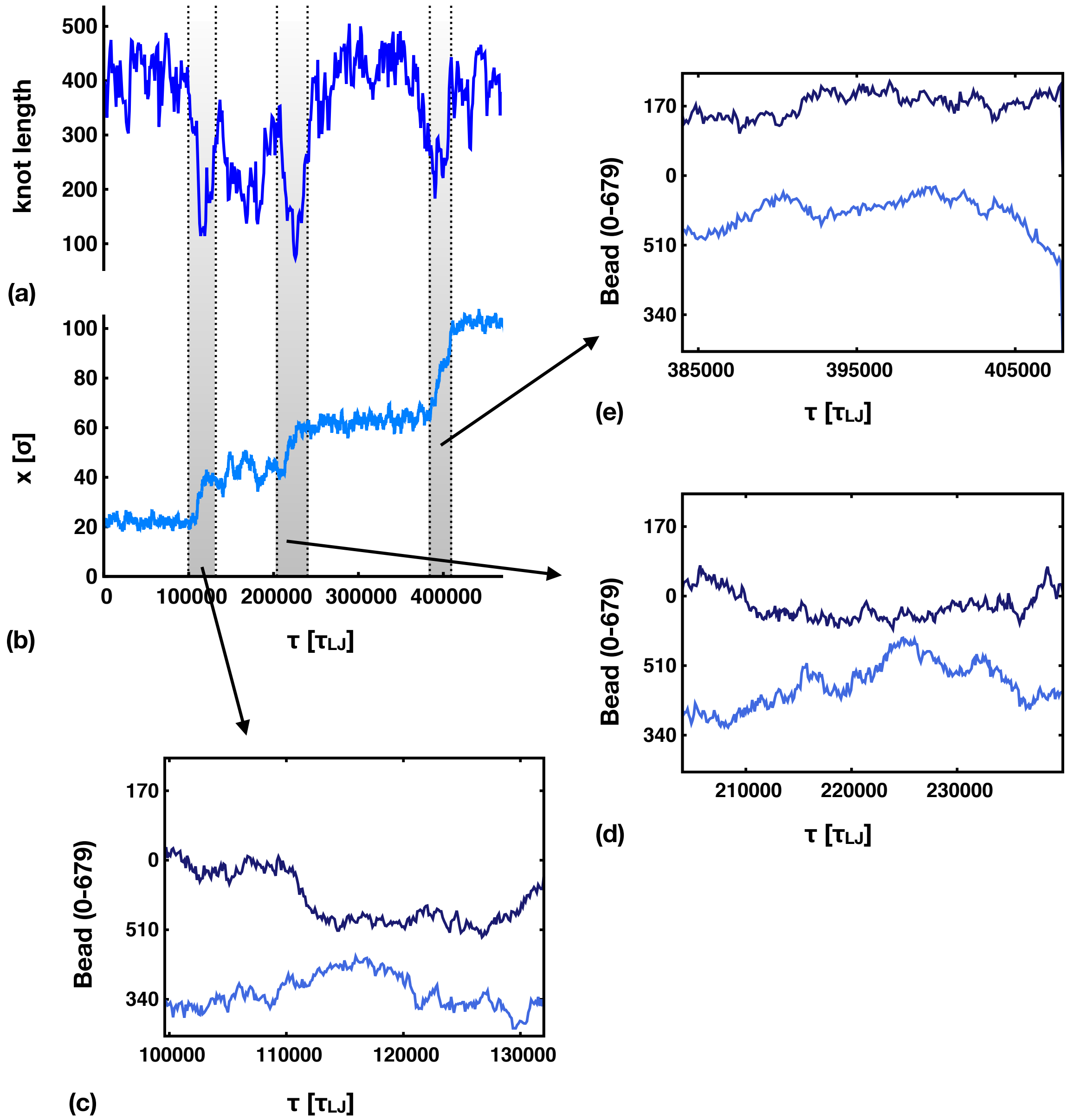

FIG. S9: Time evolution of the knot length (a) and trajectory of the polymer's centre of mass (b) for a 4_1 knot of $N = 680$ beads driven across the modulated channel by a force $f = 0.0007\epsilon/\sigma$. The parameters of the modulated channel are: $R_{min} = 8\sigma$, $L_{||} = 2R_{max} = 40\sigma$. Shaded regions are the time intervals during which the ring translocates across adjacent chambers. For these intervals, the position of the knot ends along the ring contour is shown in panels (c)-(d)-(e). The position of the knot ends wraps periodically in the 0-679 range.

[1] L. Tubiana, E. Orlandini and C. Micheletti, *Prog. Theor. Phys.*, 2011, **191**, 192–204.
[2] B. Marcone, E. Orlandini, A. L. Stella and F. Zonta, *J. Phys. A: Math. Gen.*, 2005, **38**, L15–L21.
[3] L. Tubiana, A. Rosa, F. Fragiacomo and C. Micheletti, *Macromolecules*, 2013, **46**, 3669–3678.